

Melting of orientational degrees of freedom

A. Aznar, P. Lloveras^a, M. Barrio, and J.Ll. Tamarit

Departament de Física, ETSEIB, Universitat Politècnica de Catalunya, Diagonal 647,
Barcelona, 08028 Catalonia, Spain

Received 11 July 2016 / Received in final form 22 August 2016

Published online XX XXX 2016

Abstract. We use calorimetry and dilatometry under hydrostatic pressure, X-ray powder diffraction and available literature data in a series of composition-related orientationally disordered (plastic) crystals to characterize both the plastic and melting transitions and investigate relationships between associated thermodynamic properties. First, general common trends are identified: (i) The temperature range of stability of the plastic phase T_m-T_t (where T_t and T_m are the plastic and melting transition temperatures, respectively) increases with increasing pressure and (ii) both the rate of this increase, $d(T_m-T_t)/dp$, and the entropy change across the plastic transition analyzed as function of the ratio T_t/T_m are quite independent of the particular compound. However, the dependence of the entropy change at the melting transition on T_t/T_m at high pressures deviate from the behavior observed at normal pressure for these and other plastic crystals. Second, we find that the usual errors associated with the estimations of second-order contributions in the Clausius-Clapeyron equation are high and thus these terms can be disregarded in practice. Instead, we successfully test the validity of the Clausius-Clapeyron equation at high pressure from direct measurements.

1 Introduction

Orientationally disordered phases are mesophases characterized by the presence orientational dynamic disorder that may arise in molecular crystals constituted by rather isometric or small molecules linked by weak interactions. Activation of the orientational degrees of freedom from the completely ordered crystalline phase occurs across a first-order transition with unusual large enthalpy and entropy changes that exceed those associated with the melting towards the liquid phase [1, 2]. This has made them promising as solid-state thermal energy storage materials [3, 4].

Beyond this fundamental picture, several studies have been devoted to identify additional universal thermodynamic behavior [5–9], but with limited success. Mostly, the detected common trends are restricted to a given family of composition-related compounds only, rather than to actually general features within plastic crystals.

Interestingly, several thermodynamic correlations were noticed to be shared by a wide variety of plastic crystals [9, 10]: (i) The temperature range of stability of the

^a Corresponding author: e-mail: pol.lloveras@upc.edu

40 plastic phase, $T_m - T_t$, (where T_m and T_t stand, respectively, for the temperature at
 41 the melting and plastic phase transition at a given pressure) increases at the expense
 42 of the liquid phase when the pressure is increased, i.e. $dT_m/dp > dT_t/dp > 0$. (ii) The
 43 entropy and volume changes at T_m , ΔS_m and ΔV_m respectively, decrease with pressure.
 44 These features have been explained in terms of the relative magnitude between
 45 the rotational and diffusional energy barriers [9]. On the one hand, the existence of
 46 the plastic transition occurs provided that the activation energy of rotational degrees
 47 of freedom is low enough compared to diffusion activation. On the other hand, the
 48 latter increases more rapidly with pressure than the former, which is intuitive as pressure
 49 favors the more compact stacking. In turn, a fast increase of T_m with pressure
 50 leads to a decrease of ΔS_m . The decrease of ΔV_m with pressure can then be inferred
 51 from the Clausius-Clapeyron equation, as experimental observations indicate that.
 52 Moreover, by analyzing ΔS_m as function of T_t/T_m at normal pressure for different
 53 sets of materials, it was obtained that ΔS_m decreases with T_t/T_m , and in the limit of
 54 $T_t \rightarrow T_m$, $\Delta S_m \rightarrow R \ln 2$. A deviation from this behavior was observed, however, in a
 55 compound that differed from the rest in the nature of the intermolecular bonds [10].

56 It is clear that a full thermodynamic characterization of a pVT system requires
 57 the knowledge of the effect of pressure on the thermodynamic variables. However, to
 58 date most high-pressure theoretical and experimental studies are rather limited and
 59 have focused mainly in the determination of the T - p diagram whereas high-pressure
 60 energetic and volume data are scarce, basically due to the technical difficulties and
 61 lack of standard commercial high-pressure equipment [11–19]. Clausius-Clapeyron is
 62 then evaluated at normal pressure. Moreover, investigations have been focused on
 63 inorganic and metallic compounds whereas organic plastic phases and the associated
 64 melting of orientational degrees of freedom have deserved little attention from
 65 the high-pressure community. It is worth mentioning here recent studies [20,21] on
 66 organic crystals that have suggested that application of pressure could lead to the
 67 emergence of stronger bonds between C atoms belonging to different molecular planes
 68 that are usually stabilized through van der Waals forces or hydrogen bonds. Applied
 69 pressures were, however, much larger than those of the present work.

70 Here we report systematic high-pressure experimental data on the solid and liquid
 71 phases and related transitions in a series of composition-related plastic crystals, by
 72 means of calorimetry and dilatometry under applied hydrostatic pressure and X-Ray
 73 powder diffraction. In the first part of the present study, we use these data to check
 74 and extend the aforementioned thermodynamic correlations to an unexplored range
 75 of materials and pressures.

76 On the other hand, the traditional Clausius-Clapeyron equation for first-order
 77 phase transitions renders a simple relation between volume and entropy changes at
 78 the transition point, $dT/dp = \Delta V/\Delta S$. Close to the transition, first-order derivatives
 79 arise and other additional relations can be derived [22]:

$$\frac{dT}{dp} = \frac{\Delta V_0 + \Delta\alpha_0^*(T - T_0) - \Delta\beta_0^*(p - p_0)}{\Delta S_0 + \Delta C_{p0} \log(T/T_0) - \Delta\alpha_0^*(p - p_0)} \quad (1)$$

$$\frac{d^2T}{dp^2} = -\frac{1}{\Delta V} \frac{dT}{dp} \left[\frac{\Delta C_p}{T} \left(\frac{dT}{dp} \right)^2 - 2\Delta\alpha^* \frac{dT}{dp} + \Delta\beta^* \right] \quad (2)$$

$$\frac{d\Delta H}{dp} = \frac{dT}{dp} \Delta C_p + \Delta V - T \Delta\alpha^*. \quad (3)$$

$$\frac{d\Delta V}{dp} = \frac{dT}{dp} \Delta\alpha^* - \Delta\beta^* \quad (4)$$

83 where C_p is the specific heat capacity, and $\alpha^* = (dV/dT)_p$ and $\beta^* = -(dV/dp)_T$
84 are related to isobaric thermal expansion and isothermal compressibility, although
85 the lack of the $1/V$ factor recommends a star superscript to avoid confusion. In turn,
86 the increments (Δ) refer to the difference between the quantities in either side of the
87 transitions and the zero subscript (0) to the normal pressure condition. Equation (1)
88 should then be approximately valid only in a T - p range close to normal pressure where
89 the quantities appearing in the right hand side of the equation are considered to be
90 constant. Strictly at normal pressure, Clausius-Clapeyron relation is recovered.

91 These equations have been largely disregarded, basically due to the lack of data,
92 so that studies addressing them are very rare [23]. Therefore, the second part of the
93 present work is aimed at taking advantage of the compilation of own and literature
94 data to (i) check the traditional Clausius-Clapeyron equation evaluated at high pres-
95 sure, and (ii) to obtain orders of magnitude for the above quantities and related
96 Equations (1-4).

97 2 Samples and experimental methods

98 Among plastic crystals, here we focus on a series of alcohol, amine and nitrite
99 derivatives of Neopentane $[C(CH_3)_4]$ obtained by substitution. In particular we
100 study neopentyl alcohol [with acronym NPA, chemical formula $(CH_3)_3C(CH_2OH)$],
101 neopentylglycol [NPG, $(CH_3)_2C(CH_2OH)_2$], 2-amino, 2-methyl, 1,3 propane-
102 diol [AMP, $(NH_2)(CH_3)C(CH_2OH)_2$], tris(hydroxymethyl)-aminomethane [TRIS,
103 $(NH_2)C(CH_2OH)_3$], 2-methyl, 2-nitro propane [MN, $[(NO_2)C(CH_3)_3]$ and 2-methyl,
104 2-nitro, 1-propanol [MNP $(NO_2)(CH_3)_2C(CH_2OH)$]. These compounds have been
105 extensively studied [1, 2, 9, 24-28] but thermodynamic data under pressure are rather
106 scarce.

107 Powdered NPA, NPG, MN, MNP (99% purity) and TRIS (99.9 % purity), were
108 purchased from Sigma-Aldrich, and used as such. Powdered AMP was purchased from
109 Fluka with a purity of 99.5% and used as such. Experimental methods and devices
110 used for X-Ray powder diffraction (XRPD), Differential Scanning Calorimetry at
111 normal pressure (DSC), and High-Pressure Differential Thermal Analysis (HP-DTA)
112 up to 300 MPa are the same as those described elsewhere [9]. For the HP-DTA up
113 to 600 MPa, a high-pressure cell model MV1-30 was acquired from the Institute of
114 High Pressure Physics of the Polish Academy of Science (Poland), with a temper-
115 ature range from 193 K to 393 K. Here, the samples were encapsulated in the same
116 way as used in the other HP-DTA cells whereas the calorimetric signal between sam-
117 ple and reference was obtained by attaching the encapsulated samples to a peltier
118 module, instead of using thermocouples in the Bridgman's piston setup. Another
119 peltier module was used for the reference (that was left empty), and both peltiers
120 were connected in opposition. As a usual procedure in calorimetry, heating rates were
121 approximately $2 K min^{-1}$, although in some extreme temperatures the rates could
122 be different. Dilatometry measurements in isothermal conditions were performed in
123 a custom-built device similar to that described in Reference [29], allowing pressures
124 from 0 to 300 MPa.

125 Analysis of the voltage peaks in HP-DTA curves permits the evaluation of tran-
126 sition temperatures, and enthalpy and entropy changes. The latter two require cali-
127 bration of the HP-DTA signal. On the one hand, the sensitivity of the calorimetric
128 cell is calculated from HP-DTA analysis of the solid-to-solid transition characteristics
129 of three Cu-Al-based alloys, which are assumed to be insensitive to the application
130 of hydrostatic pressure. On the other hand, the normal-pressure value obtained in HP-
131 DTA is forced to match the value from DSC. Measurements obtained by XRPD and
132 dilatometry render volume changes and related quantities such as isothermal com-
133 pressibility and isobaric thermal expansion.

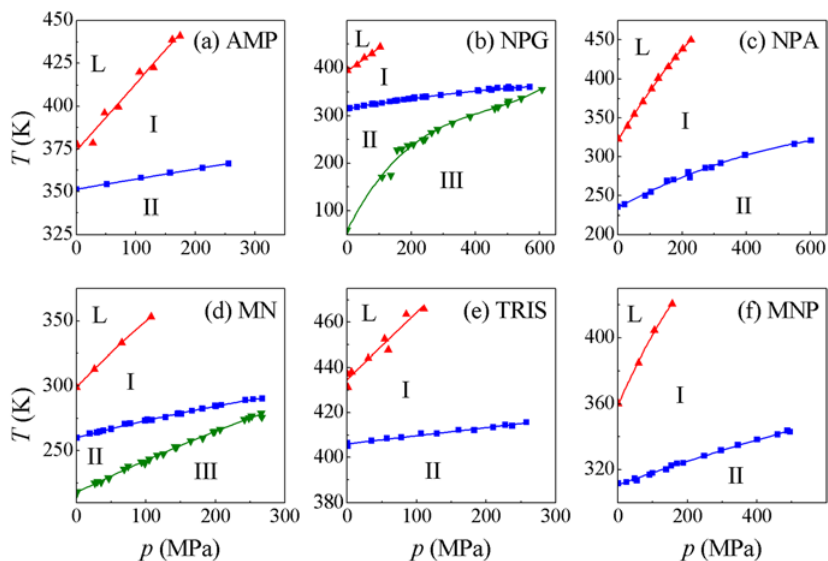


Fig. 1. T - p phase diagrams for the neopentane derivatives. In all cases, there is an increase of the temperature range of stability of the plastic phase (denoted by I) as the pressure increases.

134 It is worth discussing about the error associated with the experimental methods
 135 used in this work. Although the precision of the techniques may be relatively high
 136 ($\varepsilon(T) \sim 1$ K, $\varepsilon(p) \sim 1$ MPa, $\varepsilon(V) \sim 1\text{cm}^3\text{mol}^{-1}$), there are several major sources
 137 of error that decrease significantly the accuracy of the obtained results. In a very
 138 first step, the compound characteristics may depend on the particular sample, as the
 139 purity and the sample preparation does. In calorimetry experiments in alloys, for
 140 instance, it is known that the presence of inhomogeneities may result in anomalies
 141 in the calorimetric signal [30]. Moreover, here it is worth mentioning the error com-
 142 ing from the calibration process and the peak integration after baseline subtraction.
 143 This may explain the significant difference between the magnitude of thermodynamic
 144 quantities reported in the literature as, for instance, it is the case of the specific heat
 145 change ΔC_p across the plastic transition in NPG [31–33]. High-pressure experiments
 146 entail less accurate experimental data, with the presence of higher noise that compli-
 147 cates the choice of appropriate baselines. Moreover, some thermodynamic quantities
 148 require intermediate numerical steps (fits, derivatives, etc.) that may decrease dra-
 149 matically the accuracy of the calculated magnitudes. For instance, here $\Delta\alpha^*(p)$ must
 150 be estimated as the difference between derivatives of numerical fits from thermal data
 151 obtained in dilatometry measurements. Hence, we can only assure relative errors ε_r
 152 lower than or similar to 1% in dT/dp and lower than 10% in ΔS_0 . For most of the
 153 remaining experimental magnitudes, ε_r are estimated to be around 10–20% whereas
 154 in second-order terms, such as $\Delta\beta^*$ or $\Delta\alpha^*$, ε_r can be much larger as discussed.
 155 Having said that, for the sake of clarity we will omit error bars in the figures.

156 3 Results

157 *Calorimetric results*

158 Figure 1 reports the temperature-pressure phase diagrams for the compounds under
 159 analysis obtained by HP-DTA. From now on, L, I, II and III will refer to liquid,

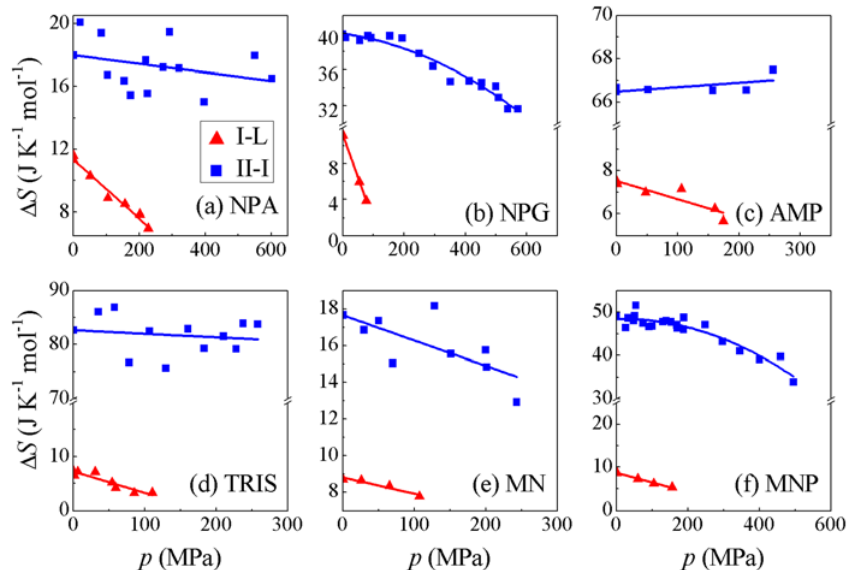


Fig. 2. Entropy change across the melting (ΔS_m , red symbols) and plastic transitions (ΔS_t , blue symbols) for the compounds under study as function of pressure. Lines are fits to the data.

160 plastic, and one and subsequent completely ordered crystalline phases respectively.
 161 Melting data for MN in this and following figures have been taken from literature [34]
 162 for completeness. Most of our data is consistent within error with literature data at
 163 normal pressure [1–4, 35–37]. However, partial disagreement has been found in few
 164 cases [2] as for instance, the melting transition for TRIS, most likely due to less
 165 accurate measurement technique based on a metabolemeter, compared to that used
 166 here.

167 Figure 2 shows the molar entropy change across the melting (ΔS_m) and plastic
 168 (ΔS_t) transitions for each compound. Red (blue) lines and symbols indicate the
 169 melting (plastic) transition. It can be observed that in all cases the temperature
 170 range of stability of the plastic phase is enlarged when the pressure is increased
 171 ($dT_m/dp > dT_t/dp$) and the entropy change on melting is lower than that associated
 172 to the plastic transition ($\Delta S_m < \Delta S_t$). We recall that this behavior is common within
 173 compounds exhibiting plastic phases, as anticipated in the introduction.

174 We can use the data fits in the previous Figures 1 and 2 to compare the behavior
 175 between different compounds, as an attempt to extract any further universal behavior
 176 within plastic crystals. This is shown in Figure 3. Figure 3(a) shows ΔS_m as function
 177 of the parameter T_t/T_m , for different compounds. This helps the understanding of
 178 Figure 3(b), where the same data is plotted for different values of pressure. There,
 179 at each pressure (for a given color), each symbol stands for one compound. Linear
 180 regressions are carried out to detect trends in the limit of $T_t/T_m \rightarrow 1$. They reveal
 181 that, while at normal pressure $\Delta S_m \rightarrow R \ln 2$, in agreement with the behavior recently
 182 reported in other sets of compounds [9], this trend is broken at high pressures.

183 Instead, Figures 3(c,d) show that $d(T_m - T_t)/dp$ is quite similar for all the com-
 184 pounds and that ΔS_t approximately does not depend on the distance between tran-
 185 sition temperatures, $T_m - T_t$. It is worth anticipating here that ΔV_t does change with
 186 pressure for all the studied compounds as it will be seen later on. It is consistent
 187 with the fact that the T - p curves for the plastic transitions exhibit non vanishing
 188 curvature, in agreement with Clausius-Clapeyron equation.

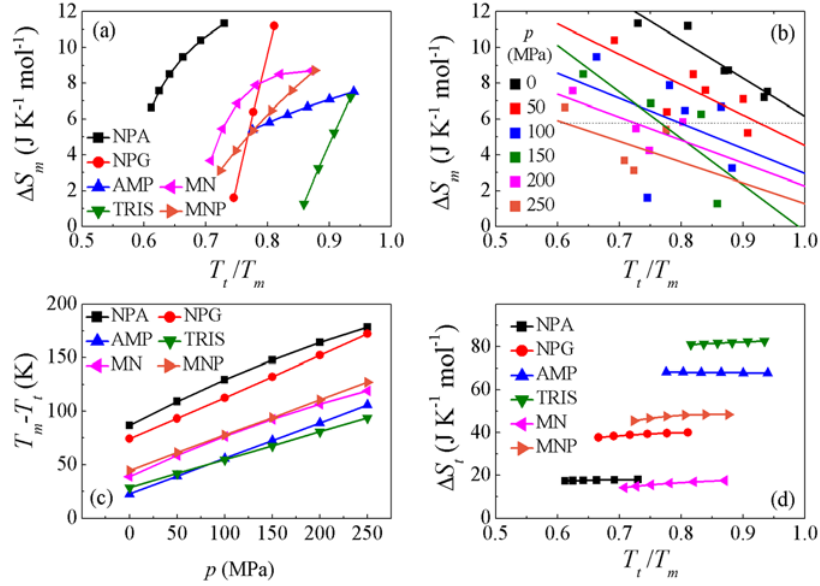


Fig. 3. (a) Entropy change on melting as function of T_t/T_m for different samples. T_t and T_m stand for plastic and melting transition temperature respectively. (b) Same data as in (a), but color code corresponds to constant pressure. (c) $T_m - T_t$ as function of pressure for different samples. (d) Entropy change at the plastic transition as function of T_t/T_m for different samples.

189 Dilatometry, X-ray powder diffraction and Clausius-Clapeyron equation

190 In this section we aim to test the Clausius-Clapeyron-related Equations (1–4) asso-
 191 ciated with the phase transitions in three of the compounds studied above, namely
 192 NPA, NPG and MN. In addition to calorimetric data presented above that provides
 193 the magnitude of dT/dp and ΔS across the transitions, the knowledge of thermal
 194 coefficients is required. For this purpose we use dilatometry and XRPD data to mea-
 195 sure the isothermal and isobaric evolution of volume respectively, which in turn will
 196 permit evaluating the thermal expansion α and isothermal compressibility β in the
 197 different phases as well as ΔV across the transitions.

198 Figure 4 shows the evolution of the volume in temperature at normal pressure,
 199 obtained by XRPD. From these data, transition volume changes ΔV and thermal
 200 expansion α at either side of the transitions can be calculated.

201 Figure 5 shows high-pressure dilatometric experimental data for NPA, NPG and
 202 MN. While for NPA and NPG we use our own experimental data, for MN we use data
 203 previously published by Jenau et al. [34]. Large discontinuous changes correspond to
 204 phase transitions. The data have been fitted to a second order polynomial, for each
 205 phase separately. From Figure 5 we can then calculate the following Figures 6–10,
 206 where we have included data taken from Figure 4 when applicable. For instance, in
 207 Figure 6 we show the volume change ΔV across the different transitions, as function
 208 of pressure, including the value at normal pressure obtained from X-ray diffraction
 209 shown in Figure 4. From linear fits (straight lines in Figure 6) we can obtain the
 210 values for $d(\Delta V)/dp$. Figure 7 shows compressibility-related values, β^* as function of
 211 pressure, obtained from the fits in Figure 5. Evaluation of this quantity close to each
 212 transition permits calculating $\Delta\beta^* = \beta_i^* - \beta_j^*$, where i and j stand for different phases
 213 at the transition, which is needed for Equations (1, 2, 4) (see Figure 8). Figure 9 shows
 214 volume–temperature data as function of temperature extrapolated from the fits in

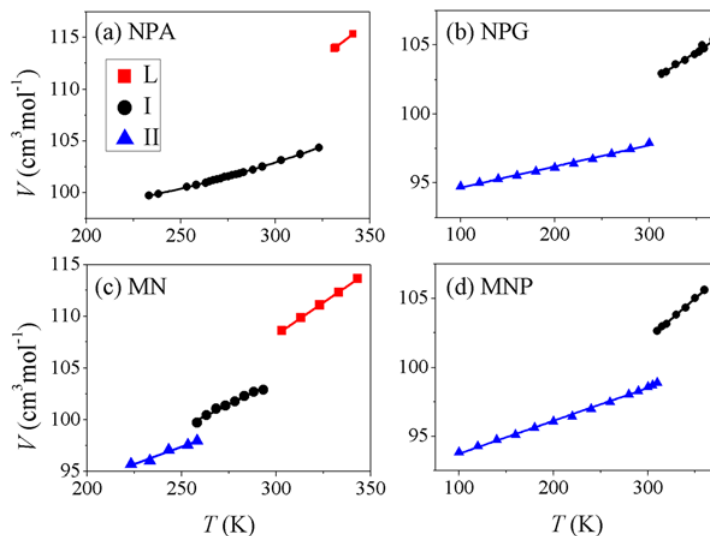


Fig. 4. X-Ray powder diffraction at normal pressure for four of the compounds under study: (a) NPA, (b) NPG, (c) MN and (d) MNP. Lines are fits to the data.

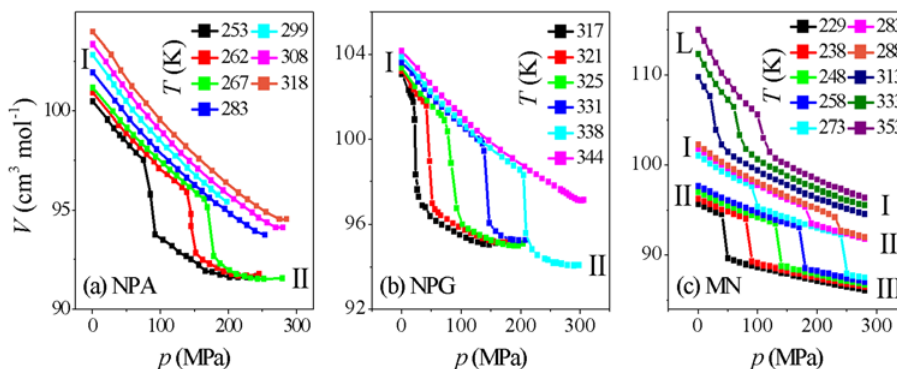


Fig. 5. Isothermal evolution of volume as function of pressure for NPA, NPG and MN. In the case of MN, the data is reproduced from Reference [34]. Phases L, I, II, and III are indicated near the corresponding regions.

215 Figure 5 for different applied pressures. Lines are linear fits to the data in all cases,
 216 as it is usually observed in organic crystals [7]. From the slopes of the linear fits, we
 217 can then extract the values for thermal expansion-related values, α^* as function of
 218 either temperature or pressure, the latter case shown in Figure 10.

219 Table 1 summarizes the data needed for Equations (1–4) for the different com-
 220 pounds. As we do not have complete data for all compounds, we will be able to
 221 evaluate the equations for NPA, NPG and MNP. Data taken from the literature is
 222 specified by different superscripts, and the corresponding references are indicated in
 223 the caption.

224 In Table 2 we compare the value for dT/dp obtained directly from experiments
 225 with that of Clausius-Clapeyron equation at normal and high pressures. It is found
 226 that the agreement is excellent. Instead, comparison to Equation (1) fails completely,
 227 indicating that Equation (1) is only valid much closer to the transition, where the

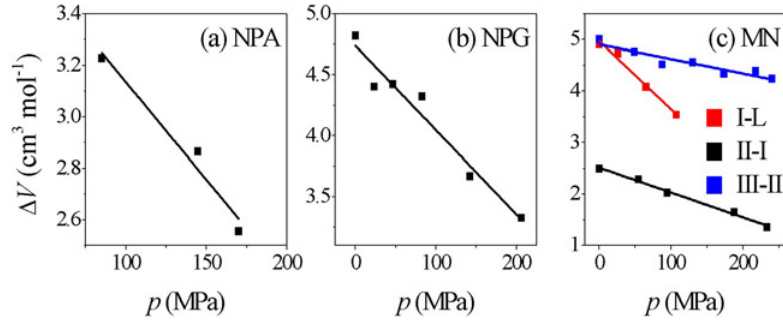


Fig. 6. Volume changes across the phase transitions as function of pressure. Values at normal pressure are taken from X-ray diffraction (see Fig. 4) whereas values under pressure are measured from dilatometry (see Fig. 5). The legend in panel (c) holds for all panels.

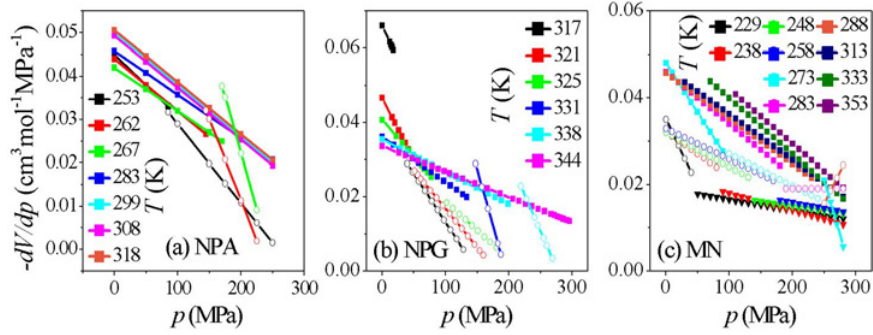


Fig. 7. Pressure derivative of volume as function of pressure, calculated from fits in figure 5. Filled squares, empty circles and downwards triangles stand for phases I, II and III respectively.

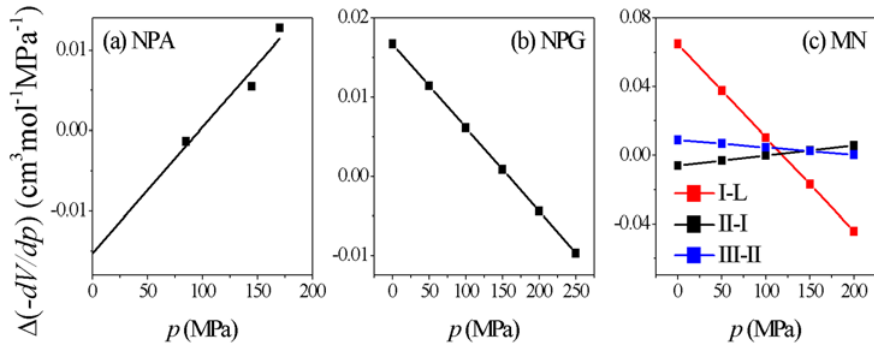


Fig. 8. Difference between pressure derivatives of volume at the transition between phases, calculated from the transition points of the fits in Figure 7.

228 magnitudes playing a role in the equation can be considered as constant, as it has
 229 been mentioned in the introduction. Indeed, Figures 6, 8 and 11 show that this valid
 230 pressure range should be restricted to few MPa. The very significant disagreement
 231 also suggests that the errors associated with these magnitudes are likely too large for
 232 a reliable estimation.

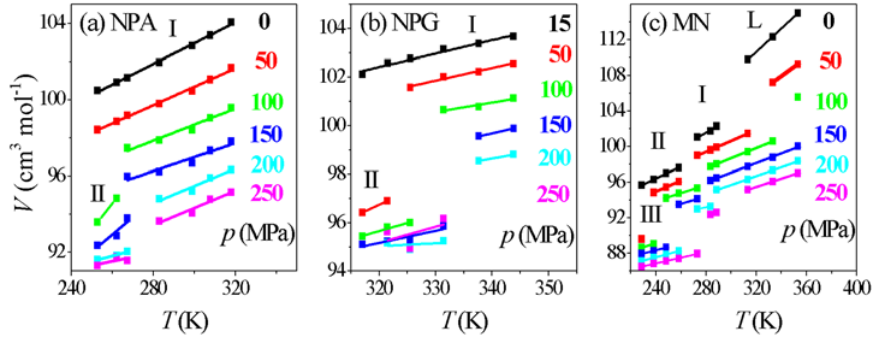


Fig. 9. Volume as function of temperature, extrapolated from Figure 5. Phases are indicated by L, I, II, III in the corresponding regions.

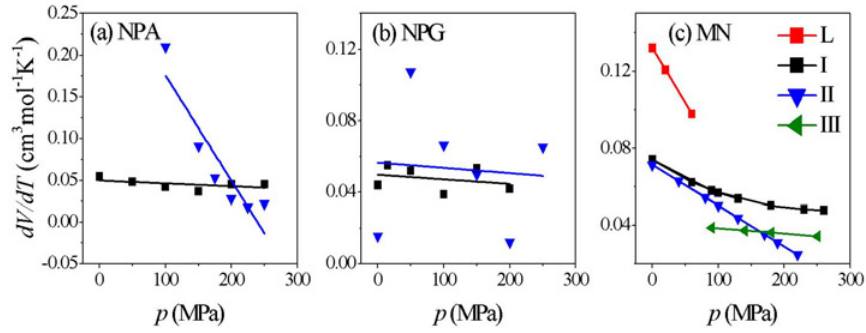


Fig. 10. Temperature derivative of volume (α^*) as function of pressure. Lines are fits to the data.

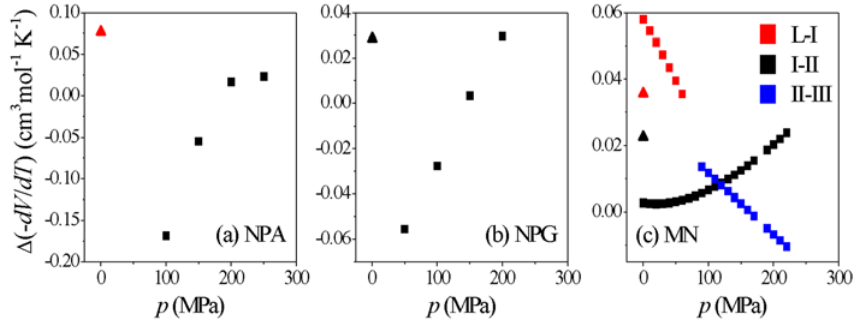


Fig. 11. Difference of α^* between phases, $\Delta\alpha^*$, as function of pressure. Square data have been calculated from data in Figure 10 whereas triangles are calculated from X-ray data (see Figure 4).

233 We then proceed to compare some thermodynamic quantities obtained through
 234 experiments with the corresponding values obtained using Equations (2–4) (see table 3). It is revealed that in general the latter values differ significantly from the
 235 former. Again, this discrepancy can be attributed to the increase of errors due to the accumulation of numerical steps necessary to infer indirectly some quantities that
 236 have not been possible to reach directly from experiments. As a consequence, this makes that the final calculated values are extremely sensitive to the initial experi-
 237 mental values. This is the case, for instance, of $\Delta\alpha^*$, that has been obtained through
 238
 239
 240

Table 1. Transition characteristics for the set of neopentane derivatives analyzed in this work. Subscript “0” refers to the values at or across the transition at normal pressure. †Taken from Reference [2]. ‡Taken from Reference [32]. *Taken from Reference [33]. #Taken from Reference [Kamae 31]. ¥Taken from Reference [38]. ?Taken from Reference [39].

		NPA	NPG	AMP	TRIS	MN	MNP
T_t at 0.1 MPa K	L-I	323.2	394.5	374.1	437.1	299.0	360.2
	I-II	235.7	314.8	351.4	406.1	260.6	311.6
dT_t/dp at 0.1 K MPa^{-1}	L-I	0.688	0.494	0.392	0.297	0.561	0.482
	I-II	0.218	0.118	0.0590	0.0361	0.141	0.0750
$d^2 T_t/dp^2$ $10^{-4} \text{K MPa}^{-2}$	L-I	-10.8	0	0	0	-10.2	-11.0
	I-II	-2.50	-1.28	0	0	-1.6	-0.339
ΔS_0 $\text{J K}^{-1} \text{mol}^{-1}$	L-I	11.3	11.2	7.52	7.21	8.7	8.71
	I-II	18.0	39.9	66.5	82.7	17.9	49.1
ΔV_0 $\text{cm}^3 \text{mol}^{-1}$	L-I	7.90 [†]	6.63 [†]	3.39 [†]	3.14 [†]	4.9	4.46 [†]
	I-II	4.01 [†]	4.82	5.06 [†]	5.07 [†]	2.5	3.90 [†]
Δcp_0 $\text{J K}^{-1} \text{mol}^{-1}$	L-I	21.5 [‡]	20.4*	26.3*	5.81*	6.71 [¥]	
	I-II		64.4 [‡] 68.9 [#] 71.8*	127*	147 [‡] 142*	-12.1 [¥]	44 [?]
$\Delta \alpha_0^*$ $\text{cm}^3 \text{mol}^{-1} \text{K}^{-1}$	L-I	0.077				0.036	
	I-II		0.029			0.023	0.035
$\Delta \beta_0^*$ $\text{cm}^3 \text{mol}^{-1} \text{MPa}^{-1}$	L- I					0.065	
	I-II	-0.015	0.017			-0.006	
$d \Delta H_0/dp$ $\text{J mol}^{-1} \text{MPa}^{-1}$	L-I	-2.2	-38	-0.95	-18	1.3	-5.8
	I-II	1.5	1.7	4.0	-0.23	-3.0	4.6
$d \Delta V_0/dp$ $\text{cm}^3 \text{mol}^{-1} \text{MPa}^{-1}$	L-I					-0.013	
	I-II	-0.0076	-0.0069			-0.0048	

Table 2. Comparison between experimental fits and calculated values for dT/dp (K MPa⁻¹) at several pressures. For pressures higher than 0.1 MPa, calculations of eq. (1) are also considered.

p (MPa)		NPA	NPG	MN
0.1	experimental	0.218	0.118	0.141
	Clausius-Clapeyron	0.217	0.118	0.141
50	experimental	0.206	0.112	0.131
	Clausius-Clapeyron	0.197	0.111	0.130
	Equation (1)	0.26	0.12	0.18
100	experimental	0.193	0.106	0.122
	Clausius-Clapeyron	0.177	0.103	0.120
	Equation (1)	0.30	0.13	0.23
200	experimental	0.168	0.093	0.102
	Clausius-Clapeyron	0.136	0.088	0.105
	Equation (1)	0.39	0.14	0.35

Table 3. Comparison between experimental and calculated values through Equations (1–4) for dT/dp , d^2T/dp^2 , $d\Delta H/dp$ and $d\Delta V/dp$ for the II-I transition at normal pressure for NPA, NPG and MN.

		NPA	NPG	MN
d^2T/dp^2 K MPa ⁻²	experimental	$-2.5 \cdot 10^{-4}$	$-1.3 \cdot 10^{-4}$	$-1.6 \cdot 10^{-4}$
	Equation (2)	$8.3 \cdot 10^{-4}$	$-3.1 \cdot 10^{-4}$	$7.4 \cdot 10^{-4}$
$d\Delta H/dp$ J mol ⁻¹ MPa ⁻¹	experimental	1.5	1.7	-3.0
	Equation (3)	4.0	3.9	-5.7
$d\Delta V/dp$ cm ³ mol ⁻¹ MPa ⁻¹	experimental	$-7.6 \cdot 10^{-3}$	$-6.9 \cdot 10^{-3}$	$-4.8 \cdot 10^{-3}$
	Equation (4)	$15 \cdot 10^{-3}$	$-13 \cdot 10^{-3}$	$9.1 \cdot 10^{-3}$

241 differences of derivatives of data which in turn are calculated by fitting experimental
 242 data. We can then conclude that in the absence of high-quality direct experimental
 243 data, Equations (1–4) do not seem useful to determine any thermodynamic quantity,
 244 as traditional Clausius-Clapeyron does. We therefore discarded to extend the
 245 calculations of these equations to higher pressures or other transitions.

246 4 Conclusions

247 By means of calorimetry, thermometry, dilatometry and X-ray diffraction, we have
248 characterized the melting of orientational degrees of freedom at high pressure in a
249 series of neopentane derivatives. We found that these composition-related compounds
250 show that (i) the slope of the differences between the $T - p$ plastic-liquid and solid
251 II-plastic transitions, $d(T_m - T_t)/dp$, is roughly independent of the compound, and
252 (ii) at low-pressure the entropy change at the solid II-plastic transition is almost inde-
253 pendent of pressure, in contrast to the volume change at the transition, that decreases
254 notably when increasing pressure. This results in slightly convex curvature of the $T-p$
255 solid II-plastic transition line in most of the compounds. This behavior is consistent
256 with Clausius-Clapeyron equation evaluated at high pressures. The present work rep-
257 represents one of the very few complete studies on the pressure-temperature dependence
258 of entropy and volume in organic plastic crystals, and shows that some universal be-
259 havior might emerge for plastic phases. It should inspire similar work in other plastic
260 crystals to confirm the observed trends as a generality beyond neopentane derivatives.

261 This work was financially supported by the Spanish Government, project No. MINECO
262 FIS2014-54734-P, and by the Generalitat de Catalunya, project No. 2014SGR-00581.

263 References

- 264 1. E. Murrill and L. Breed, *Thermochim. Acta* **1**, 239 (1970)
- 265 2. J.Ll. Tamarit, B. Legendre, J.M. Buisine, *Mol. Cryst. Liq. Cryst.* **250**, 347 (1994)
- 266 3. D.K. Benson, W. Burrows, J.D. Webb, *Sol. Energy Mater.* **13**, 133 (1986)
- 267 4. M. Barrio, J. Font, D.O. López, J. Muntasell, J.Ll. Tamarit, *Sol. Energy Mater. Sol.*
268 *Cells*, **27**, 127 (1992)
- 269 5. T. Clark, M.A. McKervey, H. Mackle, J.J. Rooney, *J. Chem. Soc., Faraday Trans. 1*
270 (1974)
- 271 6. T. Clark, T. Mc. O. Knox, H. Mackle, M.A. McKervey, *J. Chem. Soc., Faraday Trans.*
272 **173**, 1224 (1977)
- 273 7. G.J. Kabo, A.A. Kozyro, M. Frenkel, A.V. Blokhin, *Mol. Cryst. Liq. Cryst.* **326**, 333
274 (1999)
- 275 8. M.B. Charapennikau, A.V. Blokhin, A.G. Kabo, G.J. Kabo, *J. Chem. Thermodynamics*
276 **35**, 145 (2003)
- 277 9. J.Ll. Tamarit, I.B. Rietveld, M. Barrio, R. Céolin, *J. Mol. Struct.* **1078**, 3 (2014)
- 278 10. J. Reuter, D. Büsing, J. Ll. Tamarit, A. Würflinger, *J. Mater Chem.* **7**, 41 (1997)
- 279 11. M. Barrio, P. de Oliveira, R. Céolin, D.O. López, J.Ll. Tamarit, *Chem. Mater.* **14**, 851
280 (2002)
- 281 12. Ph. Negrier, L.C. Pardo, J. Salud, J.Ll. Tamarit, M. Barrio, D.O. López, A. Würflinger,
282 D. Mondieig, *Chem. Mat.* **14**, 1921 (2002)
- 283 13. J.Ll. Tamarit, M. Barrio, L.C. Pardo, P. Negrier, D. Mondieig, *J. Phys.: Condens.*
284 *Matter.* **20**, 244110 (2008)
- 285 14. M. Barrio, J.Ll. Tamarit, Ph. Negrier, L.C. Pardo, N. Veglio, D. Mondieig, *New J. Chem.*
286 **32**, 232 (2008)
- 287 15. B. Parat, L.C. Pardo, M. Barrio, J.Ll. Tamarit, Ph. Negrier, J. Salud, D.O. López,
288 D. Mondieig, *Chem. Mater.* **17**, 3359 (2005)
- 289 16. R. Levit, M. Barrio, N. Veglio, J.Ll. Tamarit, Ph. Negrier, L.C. Pardo, J. Sanchez-
290 Marcos, D. Mondieig, *J. Phys. Chem. B* **112**, 13916 (2008)
- 291 17. Ph. Negrier, M. Barrio, J.Ll. Tamarit, N. Veglio, D. Mondieig, *Cryst. Growth & Des.*
292 **10**, 2793 (2010)
- 293 18. M. Woznyj, F.X. Prielmeier, H.-D. Lüdemann, *Z. Naturforsch.* **39a**, 800 (1984)
- 294 19. H.G. Kreul, R. Waldinger, A. Würflinger, *Z. Naturforsch.* **47a**, 1127 (1992)

- 295 20. P.F. McMillan, *Nature Mater.* **6**, 7 (2007). *Benzene bridges under pressure.*
- 296 21. L. Ciabini, M. Santoro, F.A. Gorelli, R. Bini, V. Schettino, S. Rauegi, *Nature Mater.* **6**,
297 39 (2007)
- 298 22. P.W. Bridgman, *Phys. Rev.* **6**, 94 (1915)
- 299 23. W. Wagner, A. Saul, A. Pruss, *J. Phys. Chem. Ref. Data* **23**, 515 (1994)
- 300 24. T. Hasebe, H. Chihara, *Bull. Chem. Soc. Jpn.* **59**, 1141 (1986)
- 301 25. J. Salud, M. Barrio, D.O. López, J. Ll. Tamarit, X. Alcobé, *J. Appl. Cryst.* **31**, 748
302 (1998)
- 303 26. J. Salud, D.O. López, M. Barrio, J.Ll. Tamarit, *J. Mater. Chem.* **9**, 909 (1999)
- 304 27. K. Arvidsson, E.F. Westrum, Jr., *J. Chem. Thermodyn.* **4**, 449 (1972)
- 305 28. K. Suenaga, T. Matsuo, H. Suga, *Thermochim. Acta* **163**, 263 (1990)
- 306 29. R. Landau, A. Würflinger, *Rev. Sci. Instrum.* **51**, 533 (1980)
- 307 30. E.K.H. Salje, *Phase Transitions in Ferroelastic and Co-elastic Crystals* (Cambridge
308 University Press, Cambridge, UK, 1990)
- 309 31. R. Kamae, K. Suenaga, T. Matsuo, H. Suga, *J. Chem. Thermodyn.* **33**, 471 (2001)
- 310 32. D. Chandra, W.-M. Chen, V. Gandikotta, D.W. Lindle, *Z. Phys. Chem.* **216**, 1433 (2002)
- 311 33. S. Divi, R. Chellappa, D. Chandra, *J. Chem. Thermodyn.* **38**, 1312 (2006)
- 312 34. M. Jenau, J. Reuter, J.Ll. Tamarit, A. Würflinger, *J. Chem. Soc., Faraday Trans.* **92**,
313 1899 (1996)
- 314 35. M. Rittmeier-Kettner, G.M. Schneider, *Thermochim. Acta* **266**, 185 (1995)
- 315 36. M. Barrio, D.O. Lopez, J.Ll. Tamarit, Ph. Negrier, Y. Haget. *J. Mater. Chem.* **5**, 431
316 (1995)
- 317 37. J. Salud, D.O. López, M. Barrio, J.Ll. Tamarit, H.A.J. Oonk, P. Negrier, Y. Haget,
318 *J. Solid State Chem.* **133**, 536 (1997)
- 319 38. S. Urban, Z. Tomkowicz, J. Mayer, T. Waluga, *Acta Phys. Pol.* **A48**, 61 (1975)
- 320 39. J. Font, J. Muntasell, *Mater. Res. Bull.* **29**, 1091 (1994)